Fawwaz T. Ulaby
Thomas F. Bush
University of Kansas Center for Research, Inc.
Lawrence, KS 66045

Monitoring Wheat Growth with Radar

A strong correlation between the radar backscattering coefficient and plant moisture content, a parameter of wheat growth, was found.

Introduction

For many years the problem of feeding the world's expanding population has concerned both the government and civilian populace. As an aid in managing our food resources certain remote sensing techniques have been implemented. At the present time most of the civilian global sensors operate in the visible or infrared portion of the electromagnetic spectrum. While these sensors

Earlier papers[1-8] have dealt with the backscattering properties of certain agricultural targets as a function of both radar parameters and target characteristics in hopes of using $\sigma°$, the radar scattering coefficient, as a target identifier and as an aid in estimating pertinent target properties. For a discussion of the relationship between target properties, system parameters, and the measured backscatter the reader is referred to Ulaby[3].

ABSTRACT: *An experiment was conducted during the late spring of 1974 to study the scattering properties of wheat in the 8-18 GHz band as a function of frequency, polarization, incidence angle, and crop maturity. Supporting ground truth was collected at the time of measurement. The data indicate that $\sigma°$, the radar backscattering coefficient, is sensitive to both radar system parameters and crop characteristics, particularly at incidence angles near nadir. Linear regression analyses of $\sigma°$ (dB) on both time and plant moisture content result in rather good correlation, as high as 0.9, with the slope of these regression lines being 0.55 dB/day and -0.275 dB/% plant moisture at 9.4 GHz at nadir. Furthermore, by calculating the average time-rate-of-change of $\sigma°$ (real units), it is found that $\sigma°$ undergoes rapid variations shortly before and after the wheat is harvested. Both of these analyses suggest methods for estimating wheat maturity and for monitoring the progress of harvest.*

have displayed many capabilities, their use is limited to cloud-free weather conditions. In studies other than remote sensing of cropland this dependence on clear weather may be tolerable, but for dynamic targets such as agricultural crops the dependence on cloud free conditions is in most cases intolerable. Because it is nearly weather independent, radar is being investigated as a sensor for agricultural land-use mapping.

Nearly 215 million hectares of the world's cultivated land (representing about 16 per cent) are planted in wheat[9]. Radar studies of wheat, however, do not seem to represent a proportionate part of the domestic research in the remote sensing of croplands. During the late spring of 1974 (May 21 through June 25) an experiment was conducted to study the backscattering properties of wheat as a function of system parameters and target

Photogrammetric Engineering and Remote Sensing,
Vol. 42, No. 4, April 1976, pp. 557-568.

557

properties. This paper presents the results of the experiment, which indicate a promising future for monitoring wheat growth with radar.

MEASUREMENT PROCEDURE

BACKSCATTER DATA ACQUISITION

The radar used in this study, the MAS 8-18 (Microwave Active Spectrometer, 8-18 GHz), is a modified version of the mobile truck-mounted spectrometer described by Bush and Ulaby[10]. Table 1 presents the pertinent system parameters.

Backscattering measurements were acquired during the period of May 21 through July 25, 1974. Data were collected for both of the like polarized (HH and VV) configurations at angles ranging from 0° (nadir) to 70° in 10° increments. These measurements were made at eleven frequencies in the 8-18 GHz range of the instrument.

Because of its FM character, the system inherently provided fading reduction by averaging in the frequency domain[11-14]. However, due to its limited resolution-cell size, it was felt that spatial averaging was also necessary. Thus, an average of 17 spatially independent measurements were made at 0°, with the number of spatial measurements decreasing to 12 at 70°. The criterion for reducing the number of spatial measurements made at the larger angles was based on the fact that, with a panchromatic system, return power variance decreases with incidence angle[12-14].

The amount of variance reduction provided by frequency averaging is a direct function of target extent (measured radially from the antenna). Target extent, however is not necessarily the physical extent of the target but may be reduced by the range resolution of the system or by the skin depth of the target. In the case of wheat it is not possible, as will be discussed later, to experimentally estimate the degree to which penetration occurs. For lack of this type of information the following approach was taken to estimate depth of penetration. The dielectric properties of several vegetation types have been measured as a function of plant moisture content by Carlson[15] at X-band. His results indicate that vegetation with 40 per cent moisture content (the average wheat moisture over the observation period) has a relative complex dielectric constant of approximately $\epsilon_w = 12.5 - j5.0$. A wheat field, however, is a mixture of dielectrics (air and vegetation) so that the effective dielectric constant of the mixture is less than that of wheat alone. Ground measurements show that the volume of wheat occupying 1.0 m³ of free space is approximately 0.1 m³. Thus, as a very crude approximation, the average effective dielectric constant of the wheat-free space mixture was taken to be

$$\varepsilon_{eff} = 0.1\, \varepsilon_w + 0.9$$

$$= 2.15 - j0.5$$

where ε_w is the relative dielectric constant of wheat, and the relative dielectric constant of free space is taken as 1.0. Making use of ε_{eff}, the average skin depth of the target was calculated to be 2.17 cm at 13.0 GHz, the center of the 8-18 GHz band. Knowing the skin

TABLE 1.

MAS 8-18 System Specifications

Type	FM-CW
Modulating Waveform	Triangular
Frequency Range	8-18 GHz
FM sweep: Δf	800 MHz
Transmitter Power	10 dBm (10 mW)
Intermediate Frequency	50 kHz
IF Bandwidth	10.0 kHz
Antennas	
Height above ground	26 m
Reflector diameter	61 cm
Feeds	Cavity backed, log-periodic
Polarization	Horizontal transmit-Horizontal receive (HH)
	Vertical transmit-Vertical receive (VV)
Effective Beamwidth	3.05° at 8.0 GHz to 1.21° at 18.0 GHz
Incidence Angle Range	0°(nadir)-80°
Calibration:	
Internal	Delay Line
External	Luneberg Lens

depth and the range resolution of the system, it is possible to estimate the frequency spacing between two independent samples of the radar return[12] according to the equation

$$\Delta f_d = \frac{150}{D} \text{ MHz}$$

where D is the target extent measured radially from the radar antenna. By dividing the system RF bandwidth, 800 MHz, by Δf_d, the decorrelation bandwidth, it is possible to determine the number of independent samples, N, averaged by the system each time a measurement was made. Multiplying N by the number of spatially independent measurements provides the total number of independent samples of the radar return after averaging. Table 2 presents 90 per cent confidence intervals for the backscattering coefficient $\sigma°$ calculated using this approach.

FIELD DATA ACQUISITION

Although described by Cihlar[16], the method of collecting and processing the ground truth presented herein will be reviewed. Soil moisture, plant moisture, plant height, and precipitation data are presented in Figure 1.

Simultaneous with the acquisition of each scattering data set, soil moisture samples were taken at several locations across the wheat field corresponding to different incidence angle ranges[17]. Although samples were taken from several depths at each location, because of skin depth considerations[4], only the data from the top two centimeters are used in the subsequent analysis. To convert from per cent moisture-by-weight to moisture-by-volume, bulk density measurements were also taken. All soil moisture data presented herein are on a volumetric basis having units of gm/cm^3. It should be noted that the measurement period (May 21-June 25) was characterized by a high mean soil moisture (0.317 gm/cm^3) with extreme values being 0.40 gm/cm^3 and 0.20 gm/cm^3.

Of particular interest is the range of variation in plant moisture during the measurement period. From Figure 1, we see that the plant moisture curve, while monotonically decreasing an average of 1.66 per cent per day, had two regions during which the plant moisture remained somewhat constant with time (May 21-31 and June 6-12). The second "plateau" in the plant moisture curve may have been caused by the heavy precipitation recorded during the noted period.

Perhaps of more importance is the ripening process, the mechanism responsible for this consistent decrease in plant moisture. Although decreasing plant moisture is one measurable consequence of the ripening of the wheat, there are certainly other changes occurring which may not be readily measured. Thus we should bear in mind that, while consistently decreasing plant moisture may be indicative of the maturation process, there are certainly other physiological and morphological processes occurring.

DISCUSSION OF RESULTS

Because of the quantity of multi-

TABLE 2. NUMBER OF SPATIALLY DISCRETE MEASUREMENTS WITH 90% CONFIDENCE INTERVALS OF $\sigma°$(db) OF WHEAT

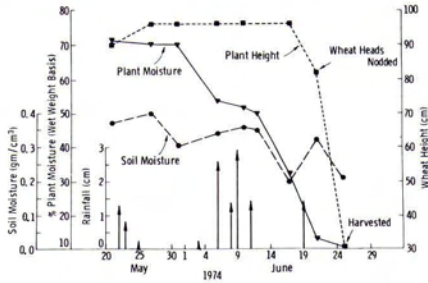| Incidence Angle	Number of Spatially Independent Measurements	90% Confidence Intervals (dB)
0°	17	+1.8 −2.0
10°	16	+1.8 −2.0
20°	15	+1.1 −1.3
30°	14	+0.93 −1.1
40°	13	+0.774 −0.774
50°	12	+0.622 −0.622
60°	12	+0.457 −0.457
70°	12	+0.403 −0.403

FIG. 1. Record of soil moisture, plant moisture, plant height, and precipitation during the observation period.

dimensional data gathered during the course of the experiment, it is not at this time possible to discuss the results in their entirety. Rather, only a representative portion will be presented in the body of this paper; a more detailed version has been documented in a report by Bush and Ulaby[17].

TEMPORAL VARIATIONS OF $\sigma°$

$\sigma°$, the radar scattering coefficient, is generally a function of the geometric and dielectric properties of the target of interest. Any variation of these target properties will normally be reflected as a change in $\sigma°$. Thus, if radar is to be useful as a tool in estimating crop maturity, it must somehow respond

with a reasonable degree of sensitivity to the geometrical and electrical variations a plant undergoes during its maturation process. Among the geometric changes in wheat are variations in plant height, leaf structure, and the appearance of the wheat head. The most obvious dielectric variation is that of changing plant moisture, which is quite dramatic in the case of wheat during the final month of its maturity. Thus, while it is recognized that the variations we may observe in $\sigma°$ are a function of crop characteristics, we should also bear in mind that these plant characteristics are in turn dependent on the passage of time. Therefore, this first section on temporal variations of $\sigma°$ will serve, among other purposes, to introduce the reader to the general trends in the variations of the scattering data.

Figures 2a through 2d present the variations of $\sigma°$ with time at an incidence angle of 0° for four frequencies: 8.6, 9.4, 13.0, and 17.0 GHz. The abscissa identifies the date on which each data set was recorded. Figure 3 presents the results of a linear regression analysis of $\sigma°_H$ and $\sigma°_V$ on time, respectively, with the number of days after May 21 being the independent variable. Shown are the estimated correlation coefficients, r^t_H and r^t_V, and the slopes of the regression lines, M^t_H and M^t_V (having units of dB/day). The abscissa
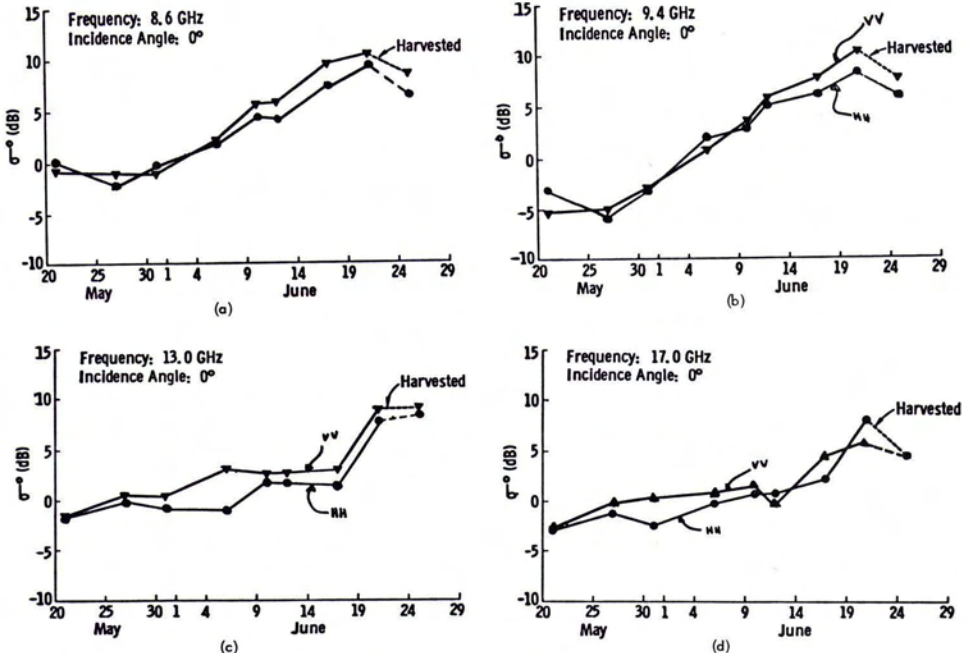

FIG. 2. Temporal variation of $\sigma°_H$ (dB) and $\sigma°_V$ (dB) as measured at 0° at (a) 8.6 GHz, (b) 9.4 GHz, (c) 13.0 GHz, and (d) 17.0 GHz.
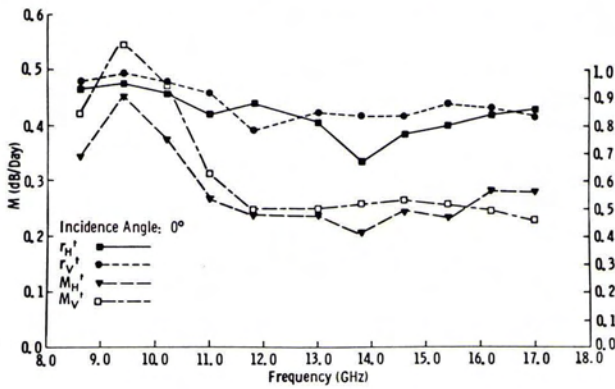
FIG. 3.   Variations of M^t_H, M^t_V, r^t_H and r^t_V with frequency.

scale is frequency in GHz. It should be noted that all regression analyses presented in this paper exclude the data set taken on June 25 since it was taken after harvest.

As a general observation it is immediately apparent that the radar is responding to the physiological and morphological changes which occurred during the final month of ripening of the wheat. At 8.6 and 9.4 GHz σ°_H and σ°_V both show an almost linear variation with time. At 13.0 and 17.0 GHz, however, this linear response is not quite as apparent although data at these higher frequencies still exhibit a dependence on the passage of time. Figure 3 presents a more complete and quantifiable representation of these trends. We note that, r^t_H and r^t_V, the estimated correlation coefficients of σ°_H and σ°_V on time, show a decreasing trend with frequency from approximately 0.95 at 8.6 GHz to about 0.85 at 17.0 GHz. This is in agreement with our earlier, more general observation, that the "linearity" of the variations of σ° with time undergo a certain amount of degradation as frequency is increased. Certainly, however, r^t_H and r^t_V remain quite high across the 8-18 GHz band.

Of equal importance to r^t_H and r^t_V are M^t_H and M^t_V. These values represent the slope of the regression lines and may be interpreted as a measure of the sensitivity of σ° to the passage of time. Obviously a very high correlation coefficient is useless in a practical sense if the sensitivity of σ° to temporal changes is small. The response of M^t_H and M^t_V to frequency (Figure 3) shows a very interesting phenomenon near 9.4 GHz. At this frequency M^t behaves in a somewhat "resonant" manner, with M^t_V being more pronounced than M^t_H. This suggests that at 9.4 GHz there exists a certain characteristic or combination of wheat characteristics to which the radar is particularly sensitive.

Whether these characteristics are of a molecular or geometric nature is not known, but it certainly appears to merit a considerable amount of future thought and investigation. At frequencies above 11.8 GHz the curves depicting M^t_H and M^t_V appear to be practically frequency and polarization independent.

Aside from the "resonant" phenomenon occurring at 9.4 GHz, the general increasing trend of σ° is also quite difficult to explain adequately. If the regression lines exhibited a negative slope it would be possible to argue that the phenomenon observed is due to a decreasing plant moisture content and, thus, decreasing dielectric constant of the target. Since the slope is positive, such an explanation can be discarded. A decreasing dielectric constant does, however, imply decreasing attenuation within the vegetation canopy. This decrease in attenuation within the vegetation canopy would then allow the radar to "see" more of the generally wet underlying soil, resulting in an increasing σ°. Although this may be a partial explanation of the phenomenon, it does not seem to be entirely consistent with the observed data or with the approximated skin depth. Consider, for example, the increase in σ°_V by about 1.8 dB between June 12 and June 17 during which time the soil moisture decreased from 0.35 to 0.20, which clearly indicates no response to soil moisture variations. Furthermore, it does not seem likely that either the "resonance" phenomenon or polarization dependence at 9.4 GHz would result from soil conditions alone. Also, the difference in M^t_H and M^t_V indicates a preferred target geometry. Visual inspection of the soil surface indicates none while the wheat itself does. The wheat was sown in rows spaced 25 cm apart such that at 0° incidence the wheat rows were oriented parallel to the E field of a

horizontally polarized signal. At a ground range of 5.3 meters (corresponding approximately to 10° incidence) the direction of the wheat rows changed by 90°. At incidence angles greater than 10° the rows were perpendicular to the E field of a horizontally polarized signal.

The results presented in Figure 2 are indeed very encouraging in terms of monitoring the progress of wheat growth. At 9.4 GHz (Figure 2b) for example, VV polarization data indicate an increase of 15.5 dB over the one month period prior to harvest, followed by a drop in return of 2.7 dB after harvest. As incidence angle is moved away from nadir, the dependence of $\sigma°$ on time appears to decrease as can be observed from Figure 4, where $\sigma°_H$ is plotted as a function of time at 13 GHz for 30° and 70° incidence angles. As a first order estimate of the $\sigma°$ sensitivity to the passage of time, Figures 5a and 5b present the slopes of the regression lines M^t_H and M^t_V and associated correlation coefficients r^t_H and r^t_V as function of frequency at 30° and 70°, respectively.

It is immediately obvious that the data at 30° contrast sharply with the data collected at nadir. We begin by noting the lack of any peaking in the M^t (Figure 5a) curves although it does appear that M^t_V and M^t_H trade roles with M^t_H being generally higher than M^t_V. Perhaps more striking, however, is the response of the correlation coefficients r^t_H and r^t_V. At 8.6 GHz we note that r^t_H indicates nearly no consistent trends of $\sigma°_H$ with time although r^t_V has a value of 0.675. However, a small increase in frequency to 9.4 GHz causes r^t_H to increase to 0.65 while r^t_V remains nearly constant. This again suggests that the choice of frequency in a rather small band around 9.4 GHz may be critical in studying the temporal variations of the scattering properties of wheat. As we further increase frequency to values above 9.4 GHz we note a marked separation in r^t_H and r^t_V with r^t_H being consistently higher. This is in contrast to the 0° correlation coefficients,
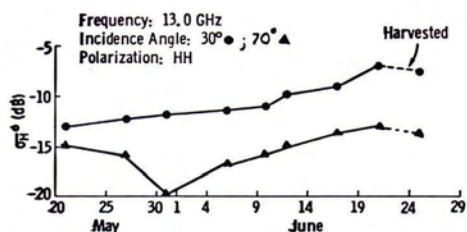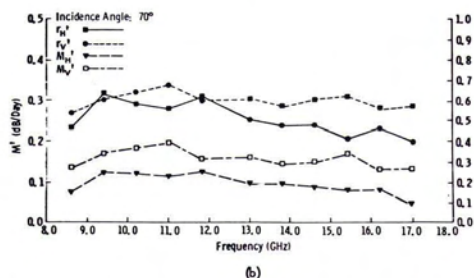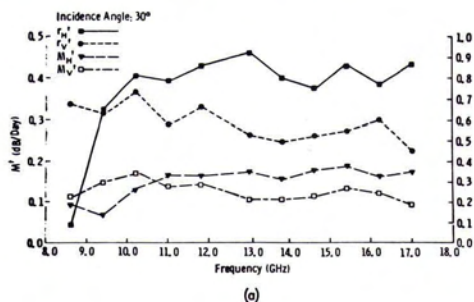

Fig. 5. Variations of M^t and r^t with frequency at (a) 30° and (b) 70°.

which showed practically no polarization dependence at frequencies higher than 11.8 GHz.

Again it is very difficult to even qualitatively explain this behavior adequately although it should be restated that the row $-\overline{E}$ field orientation has now, at 30°, changed from that of the 0° data. Let us, however, reconsider the argument that the radar is responding to changes in plant attenuation. As a rough estimate of the amount of loss expected through the wheat we might use the measured value of de Loor[18] whose data indicate that approximately 12.5 dB total attenuation should be expected at 9.3 GHz. If we are to expect this much loss at 9.3 GHz certainly the loss will increase with frequency (assuming the dielectric constant of wheat does not vary drastically with frequency) with a resulting decrease in sensitivity. Although the sensitivity factor M^t is less at 30° than at 0° we see practically no dependence of M^t on frequency above 11.0 GHz. These data also seem consistent with data presented by Lundien[19] who measured wheat at X-band for various plant heights. His data indicate a large degree of plant canopy attenuation at 0°. For an 8.9 cm stand of wheat he measured a scattering coefficient of 1.9 dB, in contrast to -15.6dB for a 73.7 cm stand. Soil moisture ranged from 15.2 to 27.7 per cent by weight. A study of wheat at other frequencies prompted his statment that "this

FIG. 4. Temporal variations of $\sigma°_H$ at 13.0 GHz as measured at 30° and 70°.

(data) suggests that the Ka-, X-, and C-band results could be used to measure vegetation parameters (height, thickness, moisture content, etc.) and that P-band frequencies may still be used for soil interrogation directly or with simple correcting factors." His statement implies that plant attenuation at higher frequencies results in a masking of underlying soil effects.

Again it can be argued that at 70° we expect a considerable amount of signal attenuation through the canopy simply due to increased path length. Thus, if we are indeed effectively measuring variations in path loss, we expect a marked reduction in the absolute values of the M^t curves. Although we do observe a small decrease in M^t_H and M^t_V as the incidence angle increases from 30° to 70° (Figures 5a and 5b), it is certainly not as great as one might expect, even at the upper end of the frequency band. Another possible mechanism responsible for the general increasing trend of $\sigma°$ with time is that of changing target geometry as the plants matured. A discussion of this mechanism will be deferred, however, to a later section.
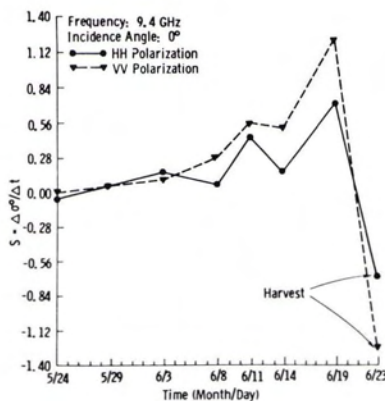
RATE OF CHANGE IN $\sigma°$

In the preceding section it was noted that the ability to monitor the ripening process of wheat was greatly influenced by the choice of radar parameters; namely frequency, polarization, and incidence angle. In this section a second approach to monitoring wheat growth will be discussed. While this approach appears to be less sensitive to system paramters, it is not intended to replace the earlier observations but rather to complement the earlier observations.

As noted earlier, the rate of change of plant moisture (one indicator of wheat maturity) did not remain constant throughout the observation period. Rather, the plant moisture sometimes remained nearly constant while at other times is decreased rapidly within a few days. Thus the question may be raised as to how the rate of change of $\sigma°$ varied during the observation period. To answer this question the following procedure was followed. For each two consecutive data sets the average rate of change of $\sigma°$ between those sets was calculated. To increase the sensitivity of these calcualtions all values of $\sigma°$ were converted from dB to real values. Thus, as an example, the rate of change of $\sigma°$ between May 21 and May 27 was calculated as follows: at 9.4 GHz, 0°, HH polarization

$$S_H = \frac{\sigma°_{H_2} - \sigma°_{H_1}}{6 \text{ days}} = -0.04/\text{day}$$

Sample results of this analysis are shown in Figures 6 and 7; different ordinate scales were used in these figures so that the relative variations of S can be seen more clearly. The abscissa values represent the date midway between the dates on which the two data sets of interest were taken. For example the value plotted as point May 24 represents the slopes of the line between sets taken on May 21 and May 27. Figure 6 presents S curves at 9.4 GHz. At 0° (Figure 6a) we note that S shows a consistent, slow increase between May 24 and June 11. Points at June 14, 19, and 23 however depart from this behavior. Of particular interest are June 19 and 23, for these represent the rate of change of $\sigma°$ shortly before and shortly after harvest.
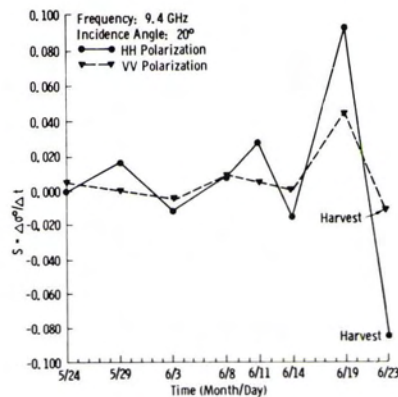
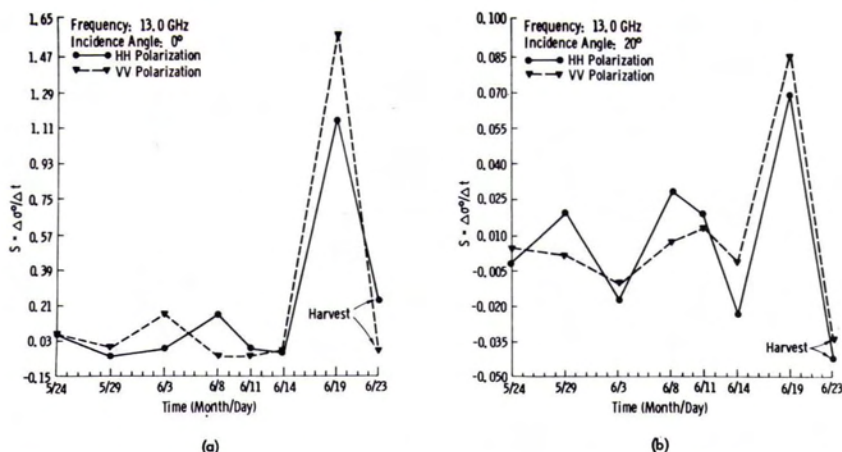FIG. 6. Rate of change of $\sigma°$ as a function of time at 9.4 GHz for (a) 0° and (b) 20° incidence angles.

FIG. 7.   Rate of change of $\sigma°$ as a function of time at 13.0 GHz for (a) 0° and (b) 20° incidence angles.

Before harvest (June 19) S increases sharply from its value on June 14 and then decreases even more markedly after harvest (June 23). It is also noted that these changes in S are greater for vertical polarization at all incidence angles observed except 20° (Figure 6b).

The effect of harvest is much more apparent in the 13.0 GHz data, particularly at 0° incidence. In Figure 7a it is seen that the variation of $\sigma°$ from day to day was apparently quite small until it was ready for harvest. During the days shortly prior to harvest, $\sigma°$ shows an extreme dependence on the passage of time, particularly $\sigma°_V$. The effect of harvest can again be clearly seen as a sharp drop in the value of S. It is noted that this trend is not quite as dramatic at angles away from nadir, although the trend is still clearly discernible (Figure 7b).

An appealing aspect of this method of interpretation is that it is independent of absolute levels of $\sigma°$. Thus it would not be necessary to calibrate (on an absolute scale) any of the existing uncalibrated imaging systems presently in operation nor would it be necessary to have a high degree of confidence in the absolute calibration of a calibrated system if such a system is used.

VARIATIONS OF $\sigma°$ WITH PLANT MOISTURE

Earlier we considered two possible causes of the increasing trend of $\sigma°$ with time. The first consideration was that the changes in plant water content (and hence dielectric constant) are directly responsible for the variations in $\sigma°$. This argument has been discarded since $\sigma°$ increases as plant moisture decreases which is contrary to what

would be expected. The second consideration is that $\sigma°$ is increasing because the radar signals are better able to penetrate the vegetation canopy as the plant moisture decreases. This argument has not yet been discarded although apparent inconsistencies have been discussed. A consideration of plant moisture as a variable can perhaps provide some insight into the mechanisms responsible for the observed phenomena.

Consider Figure 8 where $\sigma°_V$ at 9.4 GHz has been plotted as a function of plant moisture for incidence angles of 0° and 50°. We can see that $\sigma°$ is lower after harvest than before harvest even though the plant moisture decreased by only an insignificant amount. This implies that this consistent variation of $\sigma°$ is probably not due to changes
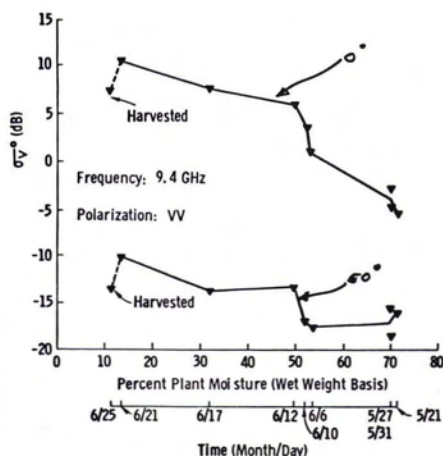

FIG. 8.   Variations of $\sigma°_V$ and r^p with frequency at nadir.

in plant moisture but rather to the dramatic change in vegetation geometry caused by the harvest. Since harvesting wheat, and thus altering plant geometry, is manifested as a change in $\sigma°$, we should consider the normal morphological changes the wheat undergoes during its ripening stages. Certainly these variations will not be as rapid and gross as those caused by harvest but they bear consideration. We begin by noting (Figure 1) that from June 6 through June 12 neither plant nor soil moisture varied to a significant degree. Plant moisture varied only 3.5 units (around 50 per cent) while soil moisture varied 0.02 gm/cm³. Thus, for all practical purposes we can consider both plant and soil moisture constant during this time. Since the electrical properties of the target were fairly constant over this period, a change in $\sigma°$ would probably imply a change in plant geometry. At both incidence angles a consistent increase in $\sigma°$ is noted during the period from June 6 through June 12, (Figure 8), the period where plant and soil moisture were fairly constant. Thus, it may be the case that these variations are due to a changing plant configuration. The most obvious geometrical change that occurred during the observation period was the appearance of the wheat heads as the plant went from a stage of vegetation growth to the reproductive stage. Of particular note is the fact that the heads appear at the tops of the plants where they are most "visible" to the scatterometer. These heads continue to develop until harvest. A second effect that occurs is the withering process the leaves undergo as they lose moisture. Hence the data

suggest that the observed variation of $\sigma°$ with plant moisture (or time) is an indirect representation of the $\sigma°$ response to changes in plant morphology.

Figure 9 presents results of a linear regression analysis of $\sigma°$ on plant moisture (excluding the data set taken after harvest). It is interesting to compare the correlation coefficients obtained by regressing $\sigma°$ on plant moisture to those obtained by regressing $\sigma°$ on time. Comparing Figures 9 with Figure 3 we see that $|r^p| \geq |r^t|$ as a general rule. This is certainly not surprising since the passage of time does not necessarily imply that the wheat is maturing whereas consistently decreasing plant moisture usually does imply a maturing crop.

The customary choice of dB units to express $\sigma°$ is usually for convenience since $\sigma°$ in real units can often vary by one or more orders of magnitude between nadir and large angles of incidence. Because plant moisture seems to be an adequate descriptor of plant maturity and because of the difficulty in quantifying plant geometry, an empirical model has been constructed describing $\sigma°$ (real units) purely in terms of plant moisture. Our discussion in the previous section indicated that linear regression analysis of $\sigma°$ (dB) on plant moisture generally provided quite satisfactory results. Hence, it was decided to express the dependence of $\sigma°$ (real units) on plant moisture in the form of an exponential

$$\sigma° = A \exp (B \cdot M_p) \qquad [\text{real units}]$$

where A and B are constants (for a given frequency-angle-polarization combination)
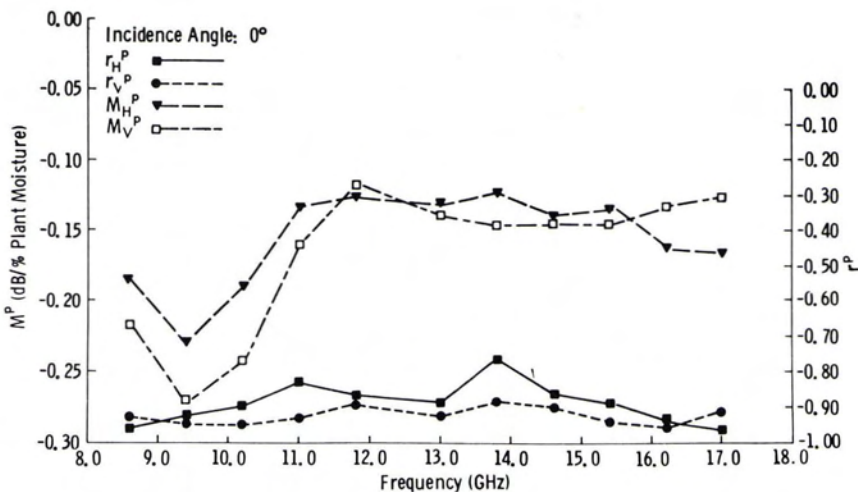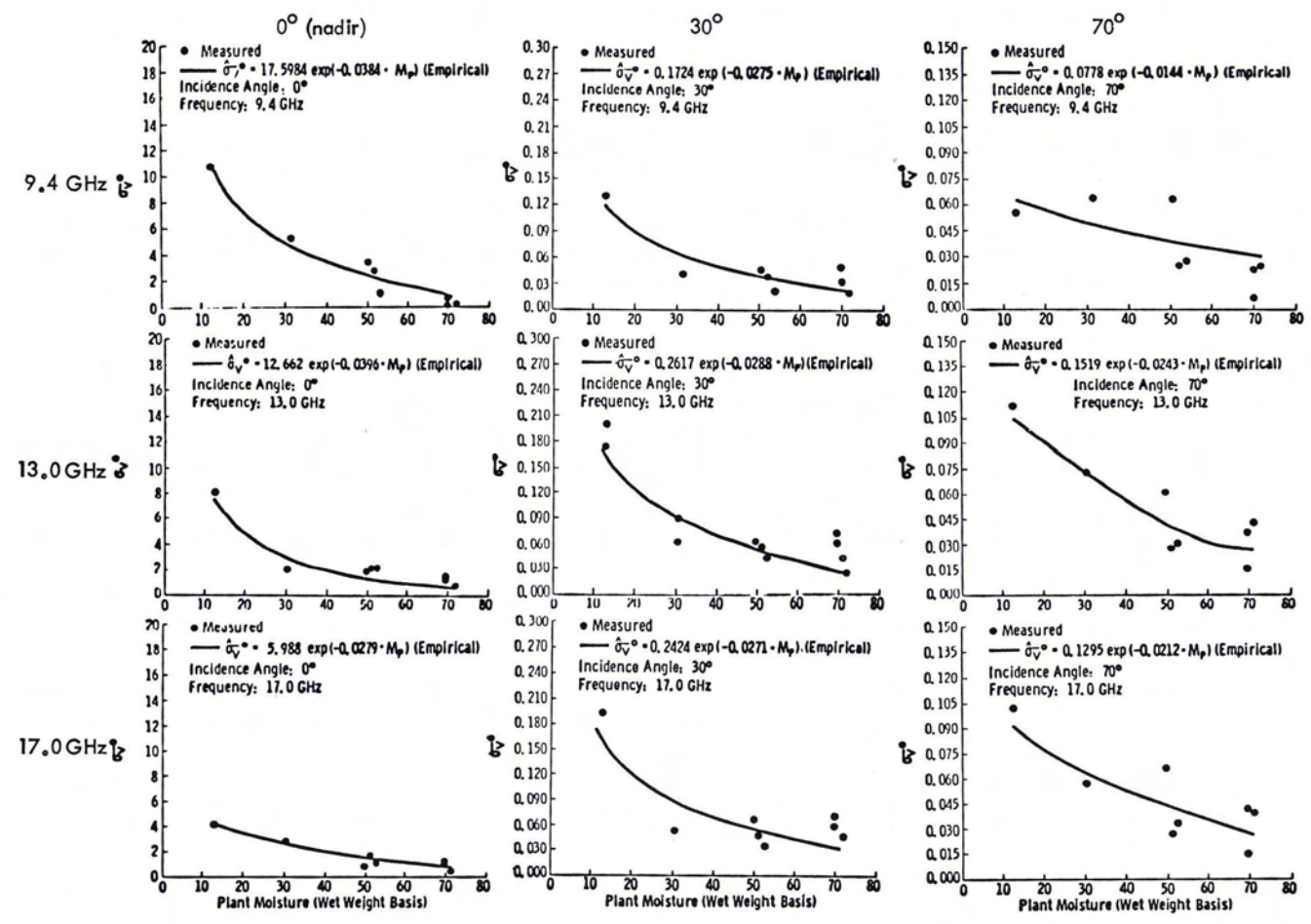

FIG. 9. Variations of M^p and r^p with frequency at nadir.

FIG. 10. Comparison of measured $\sigma°$ (real units) with empirical model at 0°, 30°, and 70° for 9.4 GHz, 13.0 GHz, and 17.0 GHz.

and M_p is plant moisture in per cent by wet weight. Using the measure $\sigma°$ (real units) and M_p values, an exponential regression equation was generated for each combination of sensor parameters.

In Figure 10 the measured data are compared to the regression curves at 9.4 GHz, 13.0 GHz, and 17.0 GHz for 0°, 30°, and 70°. Because of space considerations, only VV polarization data were chosen for presentation. In general the coefficient B, which is a measure of $\sigma°$ sensitivity to plant moisture, has approximately the same value for both polarizations at nadir but is consistently larger for VV polarization than for HH polarization at other angles. Based on a subjective judgment of the "goodness of fit" of the generated exponential curves, there does appear to be an exponential trend relating $\sigma°$ and M_p.

CONCLUDING REMARKS

Measurement of the backscattering coefficient, $\sigma°$, of wheat acquired during the final month of its growing cycle indicate that $\sigma°$ is quite sensitive to the physiological and morphological changes which wheat undergoes as it ripens, particularly during the one-week period prior to harvest. As an indicator of stage of growth, plant moisture content appears to be highly correlated with $\sigma°$, which makes radar an attractive tool for monitoring wheat growth. In terms of the range of sensor parameters examined in this study, 9.4 GHz $\sigma°_V$ nadir data show the highest sensitivity to plant moisture variations and to passage of time. At angles away from nadir, higher frequencies are found more suitable, however.

Throughout the discussion of the data presented herein it was noted that the greater majority of information was obtained from data taken at, or very near, nadir. Investigations of the ability of active microwave sensors to estimate soil moisture also indicate that incidence angles near nadir are optimum[2,4,5,6] (although at lower microwave frequencies). This is unfortunate in view of the fact that the state-of-the-art operational side-looking imaging radars perform poorest at nadir due to resolution considerations. A recent investigation by Larson et al., however, indicates "that a microwave hologram imaging radar is realizable for use on an aircraft or space vehicle"[20]. Furthermore, it is noted that the best incidence angle for optimum operation of a microwave hologram radar is near nadir. In light of the potential for radar to remotely sense croplands, such a system is very appealing.

REFERENCES

1. Ulaby, F. T., and R. K. Moore, "Radar Spectral Measurements of Vegetation," *Proceedings 1973 ASP-ACSM Joint Fall Convention*, Orlando, Florida October, 1973.

2. Ulaby, F. T., "Radar Measurement of Soil Moisture Content," *IEEE Trans on Antennas and Propagation*, vol. AP-22, no 2, March, 1974.

3. Ulaby, F. T., "Radar Response to Vegetation," *IEE Tran. on Antennas and Propagation*, vol. AP-22, no. 2, March, 1974.

4. Ulaby, F. T., J. Cihlar, and R. K. Moore, "Active Microwave Measurement of Soil Water Content," *Remote Sensing of Environment*, vol. 3, pp. 185-203, 1974.

5. Ulaby, F. T., Vegetation and Soil Backscatter Over the 4-18 GHz Region," *Proceedings of the URST Specialist Meeting*, September, 1974, Bern, Switzerland.

6. Ulaby, F. T., T. F. Bush, and P. P. Batlivala, "Radar Response to Vegetation II: 8-18 GHz Band," accepted for publication in *IEEE Trans. on Antennas and Propagation*, September, 1975.

7. de Loor, G. P., *Radar Ground Returns Part III: Further Measurements on the Radar Backscatter of Vegetation and Soils*, Physics Labortory TNO, Report No. PHL-974-05, The Hague, The Netherlands, March, 1974.

8. de Loor, G. P., and A. A. Jurriens, "The Radar Backscatter of Vegetation," *AGARD Conf. Proc. No. 90 on Propagation Limitations of Remote Sensing*, NATO, 1971.

9. Food and Agriculture Organization of the United Nations, 1972, *1972 FAO Production Yearbook*, Rome.

10. Bush, T. F., and F. T. Ulaby, *8-18 GHz Radar Spectrometer*, University of Kansas Center for Research, Inc., CRES Technical Report 177-43, Lawrence, Kansas, September, 1973.

11. Birkemeir, W. P., and N. D. Wallace, "Radar Tracking Accuracy Improvement by Means of Pulse to Pulse Frequency Modulation," *IEEE Trans. on Communications and Electronics*, pp. 571-575, January, 1963.

12. Bush, T. F., and F. T. Ulaby "Fading Characteristics of Radar Backscatter from Selected Agricultural Targets," *IEEE Trans. on Geoscience Electronics*, vol. GE-14, October, 1975.

13. Ray, H. K., "Improving Radar Range and Angle Detection with Frequency Agility," *Microwave Journal*, pp. 63-68, May, 1966.

14. Moore, R. K., and W. P. Waite, "Octave Bandwidth Microwave Spectral Response," *Photogrammetric Engineering*, pp. 1051-1053, 1973.

15. Carlson, N. L., *Dielectric Constant of Vege-*

tation at 8.5 GHz, Ohio State University, Electro Science Lab., Tech. Report 1903-5, 1976.

16. Cihlar, J., *Ground Data Acquisition Procedure for Microwave (MAPS) Measurements*, CRES Technical Memorandum 177-42, University of Kansas Center for Research, Inc., Lawrence, Kansas, July, 1973.

17. Bush, T. F., and F. T. Ulaby, *Remotely Sensing Wheat Maturation with Radar*, RSL Technical Report 177-55, University of Kansas Center for Research, Inc., Lawrence, Kansas, May, 1975.

18. de Loor, G. P., "Measurement of Radar Ground Returns,' *Proceedings of the URSI Specialist Meeting*, Bern, Switzerland, September 23-26, 1974.

19. Lundien, J. R., "Terrain Analysis by Electromagnetic Means," Technical Report No. 3-693, Report 2, U. S. Army Engineer Waterways Experiment Station, Vicksburg, Mississippi, p. 55, 1966.

20. Larson, R. W., R. W. Bayma, J. E. Ferris, M. B. Evans, J. S. Zelenka, and H. W. Doss, "Investigation of Microwave Hologram Techniques for Application to Earth Resources," *Proceedings Fifth Symposium on Remote Sensing of Environment*, University of Michigan, Ann Arbor, pp. 1521-1569, April, 1974.

BOOK REVIEW

TERRAIN ANALYSIS-A Guide to Site Selection Using Aerial Photographic Interpretation, by Douglas S. Way. (Community Development Series) Dowden, Hutchinson & Ross, Inc. Stroudsburg, Pennsylvania. Cloth Bound, 9 × 11¼, 392 pages, Illustrated, $29.50.

According to the Community Development Series Editor, Richard P. Dober, this is the first book in the Series concerned with land, the forms it takes and the capabilities it has for satisfying human needs and uses. Professor Way, the author, teaches Landscape Architecture at Harvard University and has his own related consultant business. Douglas Way Associates. He has prepared a well-organized reference work.

The book is divided into eleven chapters with a glossary, three appendixes and an index. Chap 1, "Landforms and Aerial Photographic Terrain Analysis," contains a description of how to use stereo pairs of aerial photographs with a stereoscope to perform landform analysis. It is a short chapter with many illustrations and a number of stereopairs of aerial photographs with a stereoscope to perform landform analysis. It is a short chapter with many illustrations and a number of stereopairs of aerial photographs to explain the text. Ample references for further study are given at the end of the chapter.

Chapter 2, "Processes of Physical Geology," discusses the weathering, mass wasting, and erosion of the land. Numerous illustrations and photographs are used in the text, with additional references.

Chapter 3, "Soils," contains several tables on characteristics and ratings of unified categories for roads and airfields in addition to engineering use charts and other tables and references.

Chapter 4, "Data Acquisition Sources," contains a brief description of all possible sources for obtaining aerial photography in black and white, in color, and in color infrared. Examples of radar imagery and black and white photography are shown, however, no color is given in the book. A large number of references to articles on all types of photography is given at the end of the chapter.

Chapter 5, "Issues of Site Development," is quite short and merely serves to explain some technical construction terms along with a list of references.

Chapter 6, "Sedimentary Rocks," contains a fairly detailed treatment of the different types of sedimentary rocks with many elaborate sketches and aerial photographs in stereopairs to explain each rock type. References are given at the end of each rock description.

Chapter 7, "Igneous Rocks," treats those formations in the same manner as Chapter 6. Chapter 9, "Glacial Landforms," Chapter 10, "Eolian" (Windlaid) Landforms, and Chapter 11, "Fluvian (Waterlaid) Landforms," follow the same format.

The Glossary is a fairly complete compilation of landform terms in language that is easily understood by the layman. Appendix A, "Soil Conservation Service," contains published soil surveys, Appendix B lists state geologic maps, and Appendix C lists sources for additional maps, including vegetation and topographic maps. All of the sources for maps in Appendixes B and C are indicated together with prices of the maps. The Index is complete and makes references to the text easy to locate.

Terrain Analysis is an easily readable, well-organized text book that can serve as a good beginning for basic knowledge of landforms. The text is illustrated with 395 sketches, maps, and stereopairs of aerial photographs. Although I may differ with his term of "stereo-glasses" or "stereoviewer" for what has been generally known as a stereoscope, Professor Way has produced an excellent reference book for anyone concerned with terrain analysis.

—*Abraham Anson*